PHILOSOPHICAL TRANSACTIONS OF THE ROYAL SOCIETY A MATHEMATICAL, PHYSICAL & ENGINEERING SCIENCES

On the Motion of an Elliptic Cylinder through a Viscous Fluid

G. J. Richards

Phil. Trans. R. Soc. Lond. A 1934 **233**, 279-301
doi: 10.1098/rsta.1934.0019

VI. *On the Motion of an Elliptic Cylinder Through a Viscous Fluid.*

By G. J. Richards, *A.R.C.S., B.Sc., D.I.C., Ph.D.*

(*Communicated by* L. Bairstow, *F.R.S.*)

(Received November 24, 1933—Read February 15, 1934.)

[Plates 1–3.]

Introduction.

The Navier-Poisson equations for the flow of an incompressible viscous fluid are not, as yet, amenable to complete mathematical solution. A number of approximate solutions to them have been obtained in certain special cases, the greater number of these relating to the slow steady motion of a very viscous fluid, *i.e.*, to conditions when the Reynolds' number is very small. The solution due to Stokes for the flow past a sphere is based on the assumption that the inertia terms in the viscous equations are negligible. A solution for the flow past a cylinder in the presence of walls has been obtained by Bairstow, Cave and Lang,* making the same supposition, also by Berry and Swain† for an elliptic cylinder and by Frazer‡ for a number of conditions, whilst Bassett§ obtained a solution for the flow in the neighbourhood of a sphere moving impulsively from rest. Oseen‖ derived a solution for the flow past a sphere, certain inertia terms being included in the equations solved, and the work has been extended by Lamb,¶ Frazer (*loc. cit.*), Harrison,** Filon,††‡‡ Faxen,§§‖‖ and Bairstow, Cave and Lang,¶¶ in the two-dimensional case of flow past a cylinder.

* ' Proc. Roy. Soc.,' A, vol. 100, p. 394 (1922).
† ' Proc. Roy. Soc.,' A, vol. 102, p. 766 (1922–3).
‡ ' Phil. Trans.,' A, vol. 225, p. 93 (1925).
§ ' Quart. J. Math.,' vol. 41, p. 369 (1910).
‖ ' Ark. Mat. Astr. Fys.,' vol. 4, no. 29 (1910).
¶ ' Phil. Mag.,' vol. 21, p. 112 (1911).
** ' Trans. Camb. Phil. Soc.,' vol. 23, p. 71 (1924).
†† ' Proc. Roy. Soc.,' A, vol. 113, p. 7 (1927).
‡‡ ' Phil. Trans.,' A, vol. 227, p. 93 (1928).
§§ ' Nova Acta R. Soc. Sci., Upsala,' vol. extraord., p. 1 (1927).
‖‖ ' Ann. Physik,' vol. 68, p. 89 (1922).
¶¶ ' Phil. Trans.,' A, vol. 223, p. 383 (1923).

At low speeds experimental difficulties are considerable, measurement of velocities is uncertain, and in a wind tunnel random currents would be comparable with those of the flow proper to the motion of a body. Experimental work on the resistance of a circular cylinder by RELF* supports the theoretical work due to BAIRSTOW, CAVE and LANG,† whilst WILLIAMS‡ examined the flow at low speed of glycerine past a model.

At high values of Reynolds' number, wind tunnel work attains a high degree of accuracy, and certain assumptions made by PRANDTL regarding the flow at high speeds of a fluid past a body have been successfully vindicated. These solutions relate to modified equations of motion.

In the present paper, comparison is made between the full equations of motion and experiment at a moderately low value of Reynolds' number, a partial integration of the equations being used to render the comparison practicable. The flow of water in the neighbourhood of an elliptic cylinder, at a Reynolds' number of 400, moving at a uniform speed along its major axis is analysed. The apparatus used for the experimental work was the research water tank in the Aeronautics Department of the Imperial College of Science and Technology, London. As in the Cambridge fluid motion apparatus, described in papers by MELVILLE JONES, FARREN, and LOCKYER§, and WALKER‖, a cylindrical model, whose generating lines are horizontal, is drawn through still water. The central vertical plane of the tank, at right angles to the generating lines of the cylinder, is illuminated from above, and a camera situated at the side of the tank enables photographs to be taken of the movement of particles suspended in the water in the neighbourhood of the cylinder. The exposure of the photographic plate may be made short enough for the resulting traces impressed upon it by the motion of the particles in the fluid to be treated as the instantaneous velocity vectors of the fluid, each photographic trace being assumed to define the velocity of the fluid at the mid-point of that trace; the trace made by the cylinder in the same way defines the velocity of the cylinder at the mid-instant of exposure.

Several considerations influenced the choice of 400 as the Reynolds' number at which the experiments were performed. At a high value of Reynolds' number the flow is turbulent in the wake and the differentials of velocity with respect to space, in the near neighbourhood of a body, are very large and their determination liable to considerable error. On the other hand, work at very low values of Reynolds' number would have been impossible with the apparatus, as the motion of the water itself due to convection currents and eddies would have been comparable with that produced by the moving cylinder.

* 'Aero. Res. Ctee.,' R and M, 102, p. 47 (1913–14).
† 'Phil. Trans.,' A, vol. 223, p. 383 (1923).
‡ 'Phil. Mag.,' vol. 29, p. 526 (1915).
§ 'Aero. Res. Ctee.,' R. and M. 1065, p. 54 (1926–27).
‖ 'Aero. Res. Ctee.,' R. and M. 1402, p. 97 (1931–2).

During the course of the investigation it was found that the motion was periodic in the wake, and it was assumed that the presence of such unsteadiness would not invalidate the examination of flow in the neighbourhood of the nose of the cylinder. It has also been assumed that the flow was identical with that in the neighbourhood of a similar elliptic cylinder of infinite length moving through infinite fluid, the flow at all points in the fluid being wholly in planes at right angles to the generators of the cylinder.

Mathematical Theory.

The equations of motion of an incompressible viscous fluid in two dimensions, in the absence of body forces are

$$\frac{\partial u_1}{\partial t_1} + u_1 \frac{\partial u_1}{\partial x_1} + v_1 \frac{\partial u_1}{\partial y_1} = -\frac{1}{\rho}\frac{\partial p_1}{\partial x_1} + \nu\nabla^2 u_1, \quad \ldots\ldots\ldots \quad (1)$$

$$\frac{\partial v_1}{\partial t_1} + u_1 \frac{\partial v_1}{\partial x_1} + v_1 \frac{\partial v}{\partial y_1} = -\frac{1}{\rho}\frac{\partial p_1}{\partial y_1} + \nu\nabla^2 v_1, \quad \ldots\ldots\ldots \quad (2)$$

together with the equation of continuity

$$\frac{\partial u_1}{\partial x_1} + \frac{\partial v_1}{\partial y_1} = 0, \quad \ldots\ldots\ldots\ldots\ldots \quad (3)$$

where x_1, y_1 are the orthogonal rectilinear co-ordinates of a point relative to axes with origin O at the centre of the cylinder and with directions respectively parallel to its major and minor axes, u_1, v_1 the components of fluid velocity at that point, in directions parallel to Ox_1, Oy_1 respectively, t_1 the time, p_1 the pressure in the fluid at the point (x_1, y_1), ρ the density of the fluid, and ν its kinematic viscosity. These equations together with the boundary conditions determine u_1, v_1, and p_1 as functions of x_1, y_1 and t_1.

The boundary conditions are $u_1 = 0$, $v_1 = 0$ at the boundary $\frac{x^2}{a^2} + \frac{y^2}{b^2} = 1$, where a and b are the semi-major and minor axes respectively of the cylinder, and at infinity $v_1 = 0$, and $u = -U_0$.

Eliminating the pressure from equations (1) and (2) they become

$$\frac{\partial \zeta_1}{\partial t_1} + u_1 \frac{\partial \zeta_1}{\partial x_1} + v_1 \frac{\partial \zeta_1}{\partial y_1} = \nu\nabla_1^2 \zeta_1, \quad \ldots\ldots\ldots \quad (4)$$

where

$$\zeta_1 = \frac{\partial v_1}{\partial x_1} - \frac{\partial u_1}{\partial y_1}. \quad \ldots\ldots\ldots\ldots \quad (5)$$

These equations may be transformed into a non-dimensional form. Let $x_1 = Lx$,

$y_1 = \mathrm{L}y$, $u_1 = \mathrm{U}_0 u$, $v_1 = \mathrm{U}_0 v$, $t_1 = \mathrm{T}t$, $\zeta_1 = \dfrac{\mathrm{U}_0}{\mathrm{L}}\zeta$ where L is the minor axis or breadth of the cylinder ($= 2b$) and $\mathrm{T} = \mathrm{U}_0/\mathrm{L}$, then equations (4) and (3) become

$$\frac{\partial \zeta}{\partial t} + u\frac{\partial \zeta}{\partial x} + v\frac{\partial \zeta}{\partial y} = \frac{1}{\mathrm{R}}\nabla_1^2\zeta \quad \ldots\ldots\ldots\ldots \quad (6)$$

and

$$\frac{\partial u}{\partial x} + \frac{\partial v}{\partial y} = 0 \quad \ldots\ldots\ldots\ldots\ldots\ldots \quad (7)$$

where

$$\mathrm{R} = \frac{\mathrm{U}_0 \mathrm{L}}{\nu}, \quad \ldots\ldots\ldots\ldots\ldots\ldots \quad (8)$$

and the boundary conditions become $u = 0$, $v = 0$ on the cylinder

$$\frac{x^2}{(a/2b)^2} + \frac{y^2}{0{\cdot}25} = 1,$$

and $v = 0$, $u = -1$ at infinity.

The equation of continuity (7) is satisfied by a stream function defined by

$$u = -\frac{\partial \psi}{\partial y}, \quad \text{and} \quad v = \frac{\partial \psi}{\partial x}. \quad \ldots\ldots\ldots\ldots \quad (9)$$

And if

$$\zeta = \nabla^2\psi, \quad \text{where} \quad \nabla^2 \equiv \frac{\partial^2}{\partial x^2} + \frac{\partial^2}{\partial y^2}, \quad \ldots\ldots\ldots \quad (10)$$

then

$$\frac{\partial \zeta}{\partial x} = \nabla^2 v, \quad \text{and} \quad \frac{\partial \zeta}{\partial y} = -\nabla^2 u. \quad \ldots\ldots\ldots\ldots \quad (11)$$

Now,*

$$\nabla^2 uv = u\nabla^2 v + v\nabla^2 u + 2\frac{\partial u}{\partial x}\cdot\frac{\partial v}{\partial x} + 2\frac{\partial u}{\partial y}\cdot\frac{\partial v}{\partial y}, \quad \ldots\ldots\ldots \quad (12)$$

therefore

$$\nabla^2\left\{\frac{\partial \psi}{\partial t} - \frac{1}{\mathrm{R}}\zeta + uv\right\} = 2\left\{v\nabla^2 u + \frac{\partial u}{\partial x}\cdot\frac{\partial v}{\partial x} + \frac{\partial u}{\partial y}\cdot\frac{\partial v}{\partial y}\right\}. \quad \ldots\ldots \quad (13)$$

Applying GREEN's Theorem, this equation becomes

$$\pi\left\{\frac{\partial \psi}{\partial t} - \frac{1}{\mathrm{R}}\zeta + uv\right\}_1 = \iint\left\{v\nabla^2 u + \frac{\partial u}{\partial x}\cdot\frac{\partial v}{\partial x} + \frac{\partial u}{\partial y}\cdot\frac{\partial v}{\partial y}\right\}\log r_1\, dx\, dy + \mathrm{H}_1, \quad (14)$$

where H_1 is a harmonic function, the suffix denoting the point at which the integral applies as distinct from the current point where the polar co-ordinates of the latter relative to the former are (r_1, θ), and where the integrals apply throughout the fluid.

* I am indebted to Professor L. BAIRSTOW for allowing me to apply the mathematical theory due to him.

Now

$$\left.\begin{aligned}\frac{\partial}{\partial x}\left(\frac{\partial u}{\partial x}v\log r_1\right)+\frac{\partial}{\partial y}\left(\frac{\partial u}{\partial y}v\log r_1\right)&\\ =v\log r_1\nabla^2 u+\left(\frac{\partial u}{\partial x}\cdot\frac{\partial v}{\partial x}+\frac{\partial u}{\partial y}\cdot\frac{\partial v}{\partial y}\right)\log r_1&\\ +v\left(\frac{\partial u}{\partial x}\cdot\frac{\partial}{\partial x}\log r_1+\frac{\partial u}{\partial y}\frac{\partial}{\partial y}\log r_1\right)&\end{aligned}\right\}\quad\ldots\quad(15)$$

Then (14) becomes

$$\pi\left(\frac{\partial\psi}{\partial t}-\frac{1}{\mathrm{R}}\zeta+uv\right)_1-\mathrm{H}_1=-\iint v\left\{\frac{\partial u}{\partial x}\frac{\partial}{\partial x}\log r_1+\frac{\partial u}{\partial y}\frac{\partial}{\partial y}\log r_1\right\}dx\,dy$$
$$+\int v\frac{\partial u}{\partial x}\log r_1\,dy+\int v\frac{\partial u}{\partial y}\log r_1\,dx,\quad\ldots\quad(16)$$

the line integrals being taken round the boundary. Since $\log r_1$ is the only term which depends on the position "1" the line integrals represent harmonic functions and equation (16) becomes

$$\pi\left\{\frac{\partial\psi}{\partial t}-\frac{1}{\mathrm{R}}\zeta+uv\right\}_1-\mathrm{H}'_1=-\iint v\left\{\frac{\partial u}{\partial x}\frac{\partial}{\partial x}\log r_1+\frac{\partial u}{\partial y}\frac{\partial}{dy}\log r_1\right\}dx\,dy.\quad(17)$$

As

$$\frac{\partial}{\partial x}\log r_1=\frac{1}{r_1}\frac{\partial r_1}{\partial x}=\frac{\cos\theta}{r_1}=\frac{\partial\theta}{\partial y}\quad\ldots\quad(18)$$

and

$$\frac{\partial}{\partial y}\log r_1=\frac{1}{r_1}\frac{\partial r_1}{\partial y}=\frac{\sin\theta}{r_1}=-\frac{\partial\theta}{\partial x},\quad\ldots\quad(19)$$

therefore equation (17) becomes

$$\left.\begin{aligned}\pi\left\{\frac{\partial\psi}{\partial t}-\frac{1}{\mathrm{R}}\zeta+uv\right\}_1-\mathrm{H}'_1=\iint v\frac{\partial u}{\partial y}d\theta_{y=\text{const.}}\,dy&\\ -\iint v\frac{\partial u}{\partial x}d\theta_{x=\text{const.}}\,dx\ldots&\end{aligned}\right\}\quad\ldots\quad(20)$$

$$=\iint v\frac{\partial u}{\partial y}d\theta_{y=\text{const.}}\,dy+\iint v\frac{\partial v}{\partial y}d\theta_{x=\text{const.}}\,dx\quad\ldots\quad(21)$$

or, dropping the suffixes,

$$\frac{\partial\psi}{\partial t}-\frac{1}{\mathrm{R}}\zeta+uv-\mathrm{H}=\mathrm{X}+\mathrm{Y},\quad\ldots\quad(22)$$

where

$$\mathrm{Y}=\frac{1}{\pi}\iint v\frac{\partial u}{\partial y}d\theta_{y=\text{const.}}\,dy,\quad\mathrm{X}=\frac{1}{\pi}\iint v\frac{\partial v}{\partial y}d\theta_{x=\text{const.}}\,dx.\quad\ldots\quad(23)$$

The evaluation of the integrals X and Y is discussed later. The presence of an arbitrary

function H in equation (22) is a consequence of the elimination of the pressure p_1 from equations (1) and (2). It follows that if the function H experimentally determined is harmonic, the viscous equations are satisfied. The viscous equations were brought to the form of equation (22) in order to avoid the triple differentiation of experimentally determined values of u and v which would have been necessary had equation (6) been examined.

Analysis of a number of photographs of the flow in the neighbourhood of the cylinder enabled an experimental determination of the value of H to be made. The distribution of H on a contour enclosing the ellipse (or rather its distribution on a cylindrical surface whose generators are parallel to those of the elliptic cylinder) together with the condition that H is zero at infinity defines a harmonic function (Hc) throughout the field. The agreement between Hc and the experimentally determined value of H at any point of the field thus forms a criterion of the agreement between experiment and the equations of motion for a viscous fluid. The value of H on a contour enclosing the ellipse, rather than its value on the boundary was used in the determination of the function Hc, as the values of the functions X, Y and $uv - \zeta/\mathrm{R}$ at the contour could be determined with greater accuracy, than could their values at the boundary of the cylinder.

Description of Apparatus.

The water tank, shown in figs. 1 and 2, in which the experimental work was carried out is rectangular in section, its inside dimensions being 12′ long × 1′ 6″ high × 12″

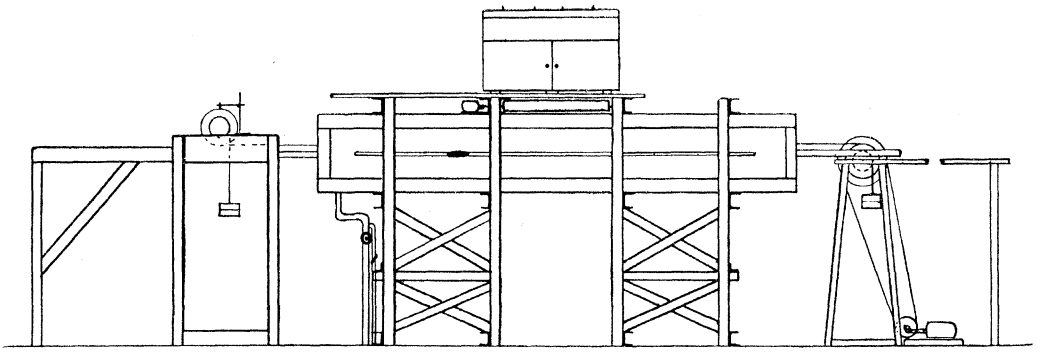

FIG. 1.—Front view of tank and driving mechanism—Scale $2\frac{1}{2}$″ to 12′.

wide. The middle side panel through which the photographs were taken measures 3′ × 16″. Movable sheets of glass which close the top of the tank when an experiment is in progress eliminate the effects of a free surface. The model, an elliptic cylinder in this work, is attached to a carriage which may be moved nearly the whole length of the tank.

The central longitudinal vertical plane of the tank is illuminated by mercury vapour lamps, contained in a case capable of sliding on rails above the tank. A lens system is provided to concentrate the light in a thin central sheet.

The elliptic cylinders, of which there were two in these experiments, have a fineness ratio of 6 to 1, the major axes (or chord) being $3\frac{3}{4}''$ and $9''$ respectively, and their lengths such that they just clear the back and front of the tank between which they move. The cylinders are of brass, being solid at one end, to give a firm attachment for the supporting spindle, whilst in the other is a conically shaped hollow, capped by a glass plate mounted in a small brass frame. Through a small hole in the top of the cylinder at its centre section, light falls from the lamps on to a platinum wire mounted at an angle of 45° to the horizontal, and lying in the vertical plane along the cylinder; light is thus reflected through the glass plate, producing a trace on a photographic plate, so that the position and velocity of the cylinder may be correlated with those of particles in the fluid.

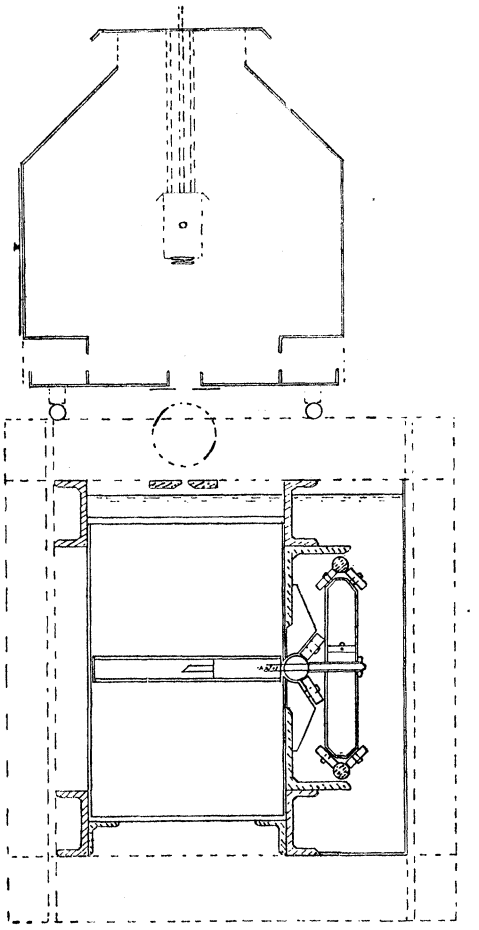

FIG. 2.—Section showing the model, carriage, and lighting system—Scale 1″ to 1′·

Fitted in front of, and close to, the lens of the camera is an electrically controlled shutter. The control is either by hand or by means of a contact fitted to the carriage carrying the model.

A revolving shutter situated above the level of the water in the tank and in the path of the beam of light from the lamps causes the particle traces on the photographic plate to appear broken into shorter tracks, this interruption increasing the accuracy with which they may be measured.

Two electromagnetic marking pens record on a strip of paper attached to a rotating drum the velocity of the model and the instant of exposure of the photographic plate.

A two-way travelling microscope is used for measuring the position, length and orientation of particle traces on a photographic plate. The microscope is fitted with a rotatable graduated head in which is a micrometer eye-piece; by means of this the orientation and length of a particle trace are measured, whilst its position is indicated by the two linear scales.

Experimental Method.

The tank was filled with water and allowed to stand all night when the large scale vortex produced on filling the tank died away, and the water attained the temperature of the room, the model having first been drawn to its starting position.

The substance used to render visible the flow of water was a mixture of unsweetened

condensed milk and absolute alcohol. This, in water, broke up into fine white particles, which diffused the light falling upon them. The actual mixing of the milk and alcohol was rather critical for if they were too well shaken a milky cloud was formed in the tank rather than a clearly defined distribution of particles, and if they were too little mixed, lumps of oily milk fell to the bottom, at the same time clouding the water. However, a large number of the particles always either rose to the top or fell to the bottom.

The effect of the particles on the kinematic viscosity of water was found to be negligible. This was determined by measuring the ratio of the rate of efflux of water carrying particles through a tube to the rate of efflux of pure water under the same conditions of pressure. Introduction of the milk particles produced a disturbance of the water but with care the eddy vorticity ensuing was small, and died away rapidly. If an attempt were made to allow the water to settle for too long a period after the particles had been formed they either became united in long tracts like fungal growths, or else they fell to the bottom leaving the liquid slightly clouded. After about four hours the residual motion became less than 0·02 cm./sec. The mercury vapour lamps were then lit, and a photograph taken of the residual motion. This was necessary as visual observation was very deceptive, the motion of the water being so small. The marking pens and rotating shutter were then set in action, and the cylinder caused to travel the length of the tank while a photograph was taken.

Measurement of all the traces in the field would have been both laborious and haphazard, owing to their random distribution; the velocity distribution along lines $x = \text{const.}$ was therefore determined. It was improbable that any trace would have been in such a position as to define the velocity at a point on a line so chosen, so that traces the centres of which were within a certain distance from such a line were taken to be indicative of the velocity at the point nearest to them on that line. The tolerance if too small did not permit of many traces being measured and if too large caused an error to be introduced into the velocity distribution determined. In a region where there were very few points, interpolation was made between two traces on either side of the line. The tolerance adopted was $\pm 0{\cdot}025$ (non-dimensional units) to either side of a line $x = c$. The magnitude and direction of fluid velocity were determined from photographs along as many lines $x = c$ as were required, and so the velocity components in the directions x and y found. To the determined value of the x component was added unit velocity -1, to change the problem to one of a cylinder at rest in a fluid moving past it with velocity -1 at infinity.

Experiments Performed.

The nature of the flow in the neighbourhood of the two cylinders was determined, each experiment being carried out at the same Reynolds' number, approximately 400. The smaller cylinder was used for the determination of the flow in the outer field and

the larger for the determination of that near to the cylinder. Fig. 3 illustrates the region of the field investigated.

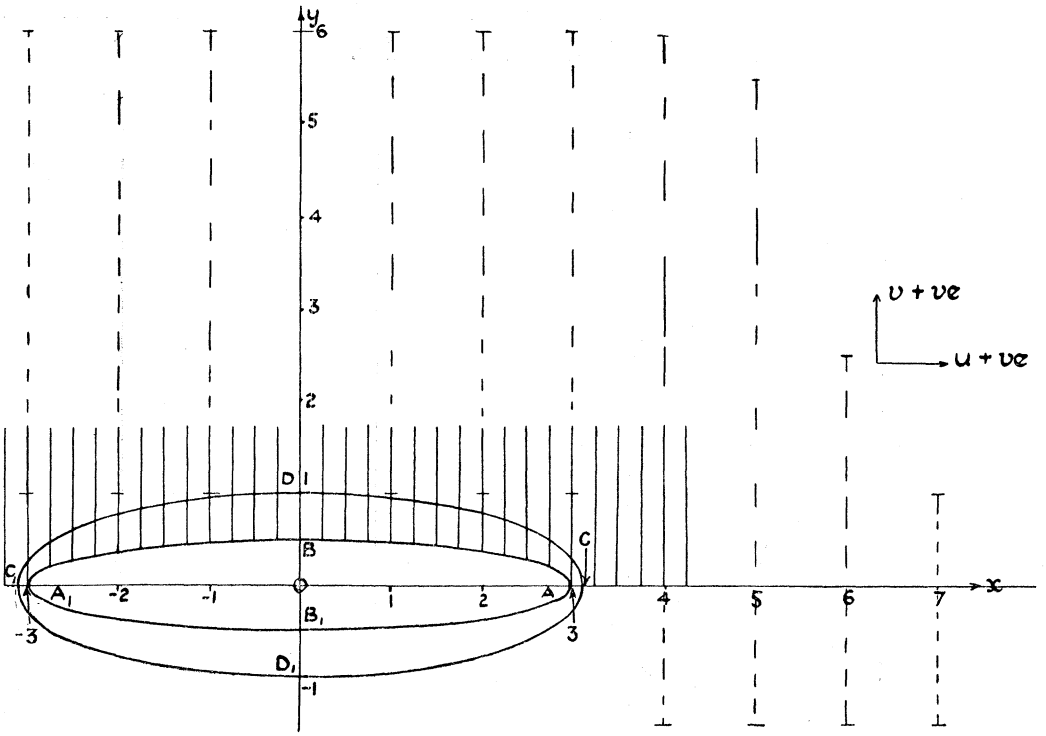

FIG. 3.—Region of field investigated. Velocity distribution determined with small cylinder along broken vertical lines; with large cylinder along full vertical lines. Boundary ellipse shown ABA_1B_1A; contour ellipse shown CDC_1D_1C.

Experimental Work with the Small Cylinder.

One photograph, fig. 11, Plate 1, of the motion of the small cylinder through water was analysed, and the velocity distribution determined along lines $x = 7, 6, 5, \ldots -2, -3$ and from approximately $y = 7$ to within 0·5 of the cylinder. The data relevant to the experiment are given in Table I, and an example chosen at random of the method of analysis of the photograph in Table II.

Experimental Work with the Large Cylinder.

Nine photographs of the flow in the neighbourhood of the large cylinder were analysed, four of the flow in front of the cylinder, two of that over its middle, and three of that behind it. The velocity distribution was examined along lines $x = 4{\cdot}25, 4{\cdot}00, \ldots -2{\cdot}75, -3{\cdot}0$, from approximately $y = 2{\cdot}0$ to the surface of the cylinder. Behind $x = -3{\cdot}0$ flow is periodic. The values of Reynolds' number at which the experiments were carried out, and the velocity of the cylinder in those experiments are given in Table I. As the velocity components at 1800 points were determined and therefore 7200 readings made it was thought that curves showing the

deduced velocity components plotted against y for various values of x would be of greater value than the tabulated results. Examples of such curves are shown in figs. 4 and 5. Photographs of the flow before, over the middle, and behind the cylinder are shown in figs. 12, 13 and 14, Plates 1 and 2.

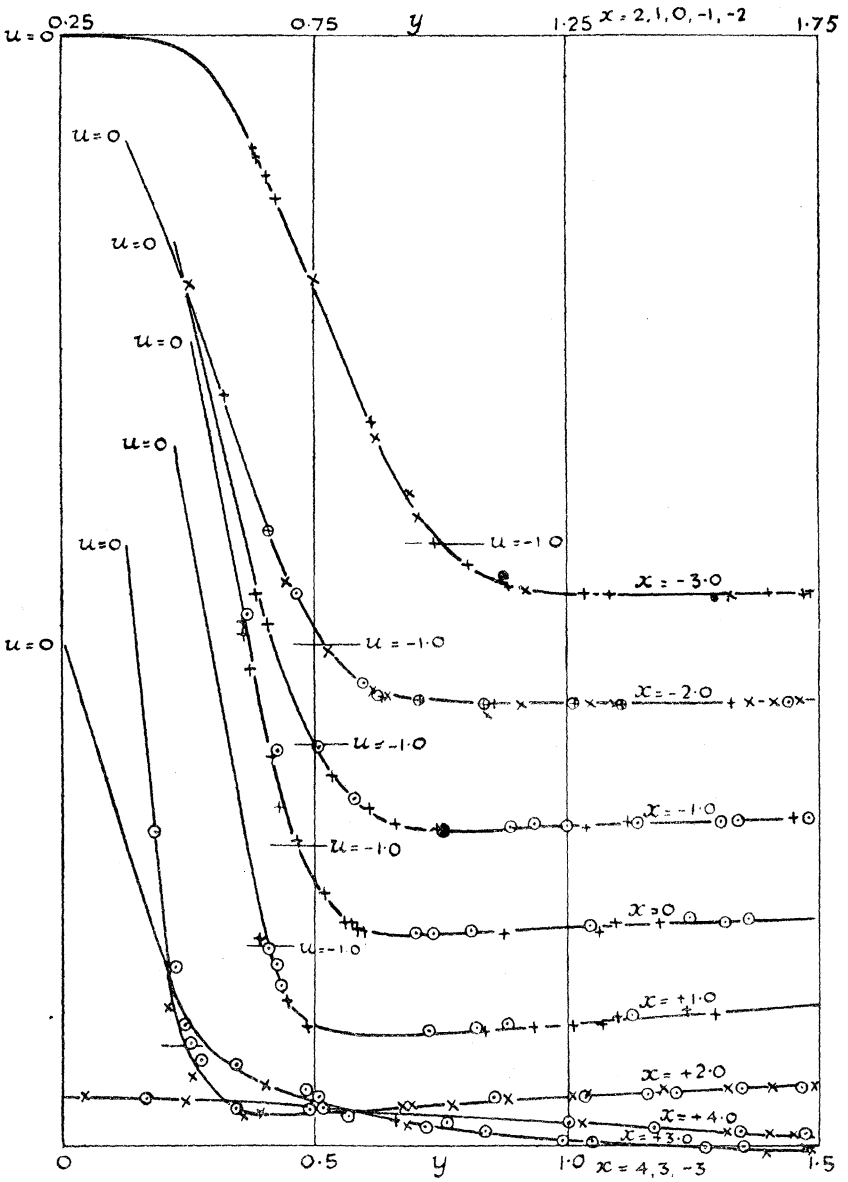

FIG. 4.—Distribution of u along lines x = constant. + Plates C 50, C 22; × C 52, C 24; • C 60, C 48; ⊙ C 40, C 54.

Also, in order to illustrate the nature of the oscillating wake two photographs, figs. 15 and 16, Plate 3, are reproduced, showing the wake at mean distances of $\frac{2}{3}$ and $3\frac{1}{3}$ chords respectively behind the cylinder.

Some measurements which have been made of this wake are being described elsewhere.

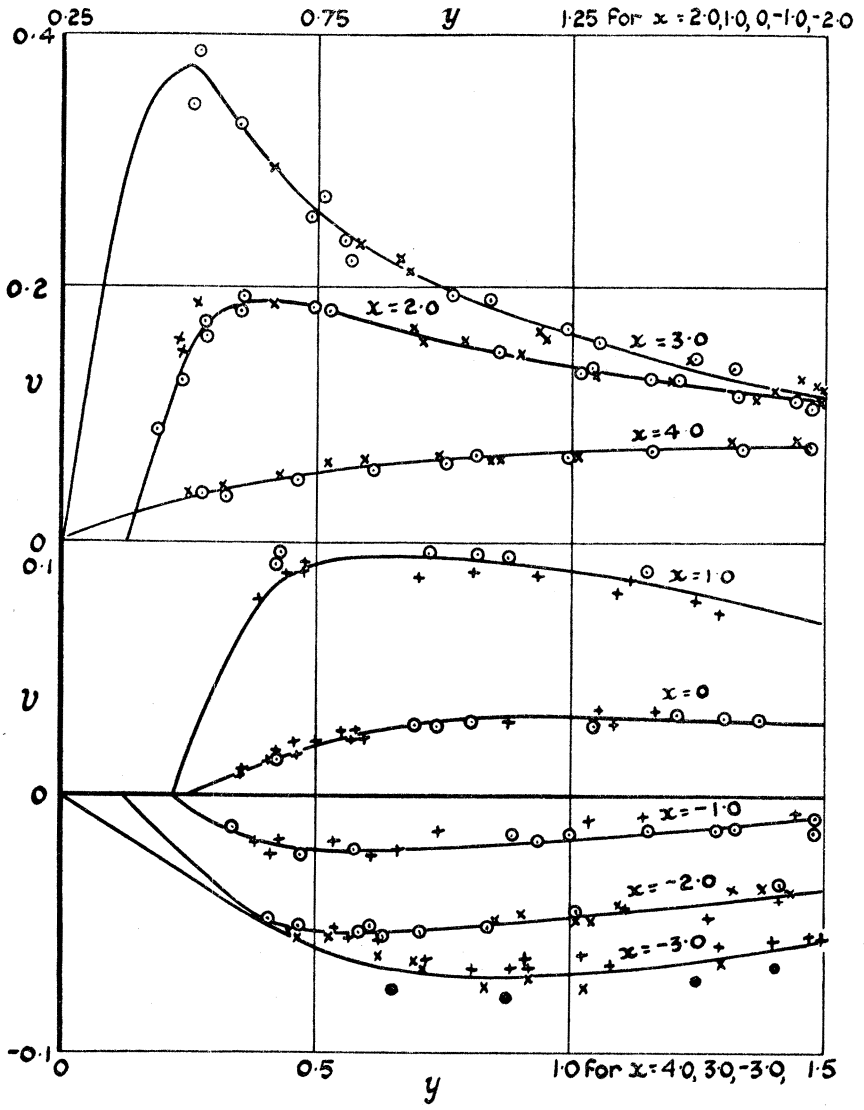

FIG. 5.—Distribution of v along lines x = constant. + Plates C 50, C 22; × C 52, C 24; • C 60, C 48; ⊙ C 40, C 54.

TABLE I.—Data Relevant to Experiments.

Plate No.	Region photographed.	Breadth of cylinder (L).	Velocity (U_0).	Kinematic viscosity (ν).	$R = U_0L/\nu$.
		cm.	cm./sec.		
A 21	Outer field	1·59	2·52	0·01096	399
C 24	Front	3·81	1·13	0·01028	413
C 48	,,	3·81	1·164	0·01122	393
C 54	,,	3·81	1·13	0·01122	381
C 56	,,	3·81	1·136	0·01122	385
C 22	Middle	3·81	1·166	0·01028	428
C 40	,,	3·81	1·096	0·01042	397
C 50	Back	3·81	1·234	0·01122	416
C 52	,,	3·81	1·218	0·01122	411
C 60	,,	3·81	1·14	0·01122	386

TABLE II.—Example of the Method of Analysis of a Photograph (A 21).

Symbols used :—

Position of particle trace with respect to the linear scales of the travelling microscope	(x', y')
Position of trace with respect to origin in non-dimensional units	$(x + h, y)$
Orientation of particle trace	$\theta°$
Readings of ends of particle traces in micrometer eye-piece	V_1, V_2
Non-dimensional length of trace	V
Distance of centre of particle trace from the chosen line $x =$ const	h cm.
Velocity components relative to fluid at rest at infinity	$(u + 1, v)$ $= V \cos \theta$, $V \sin \theta$.
Breadth of the cylinder in the photograph (the non-dimensional unit of length)	1·125 cm.
Co-ordinates of centre of cylinder at the mid-instant of exposure	8·425 and 5·43 cm.
Length of trace in terms of turns of micrometer in eye-piece	9·16

Example of the readings :—

x.	x'.	y'.	y.	V_1.	V_2.	V_2-V_1.	V.	$\theta°$.	h.	$u+1$.	v.
	cm.	cm.							cm.		
+1	9·56	6·29	0·77	3·36	4·62	1·26	0·135	43·3	+0·01	−0·099	+0·091
	9·62	6·84	1·27	3·31	4·56	1·25	0·136	39·0	+0·07	−0·106	+0·085
	9·62	7·09	1·50	3·60	4·81	1·21	0·132	38·0	+0·07	−0·104	+0·080
	9·50	7·36	1·74	3·53	4·61	1·08	0·118	37·0	−0·05	−0·095	+0·070
	9·50	8·13	2·43	3·36	4·23	0·87	0·095	41·5	−0·05	−0·071	+0·062
	9·63	8·79	3·03	3·55	4·28	0·73	0·079	30·0	+0·08	−0·062	+0·050
	9·57	9·78	3·92	2·95	3·53	0·58	0·052	36·0	+0·02	−0·046	+0·030

Analysis of Results.

The measured values of u and v were plotted against y (x being constant) and smooth curves drawn through the points. The values of u and v as given by these curves were then plotted against x (y being constant) and smooth curves again drawn. Cross plotting in this way, curves for u and v were obtained which were smooth when plotted either against x or y.

The determination of differentials, $\partial u/\partial x$, $\partial u/\partial y$, $\partial v/\partial x$, $\partial v/\partial y$ presented no difficulty. The slopes of the curves $u - x$, $u - y$, $v - x$, and $v - y$ were found mechanically and plotted against the appropriate co-ordinates; the curves were smoothed, and when integrated back the original curves were obtained. The values of

$$v\frac{\partial v}{\partial y},\ v\frac{\partial u}{\partial y},\ \zeta,$$

and uv were then determined and hence $uv - \frac{1}{R}\zeta$.

The distribution of $\frac{\partial u}{\partial x} + \frac{\partial v}{\partial y}$ was also found, and is given in Table III.

TABLE III.—$\partial u/\partial x + \partial v/\partial y$.

y \ x	7·0.	6·0.	5·0.	4·0.	3·5.	3·0.	2·5.	2·0.	1·5.
0	0	0	−0·01	+0·04	0	—	—	—	—
0·1	—	—	—	+0·04	−0·02	—	—	—	—
0·2	—	—	—	+0·02	+0·06	0	—	—	—
0·3	—	—	—	+0·02	+0·05	−0·20	−0·40	—	—
0·4	—	—	—	+0·01	+0·04	−0·30	+0·40	−0·35	—
0·5	—	—	—	0	+0·03	−0·04	+0·14	−0·01	−0·03
0·6	—	—	—	−0·01	+0·02	0	+0·03	+0·03	−0·07
0·7	—	—	—	−0·01	+0·01	0	0	+0·02	−0·02
0·8	—	—	—	0	0	0	−0·01	0	+0·01
0·9	—	—	—	0	−0·02	−0·02	−0·02	0	+0·02
1·0	0	−0·01	0	0	0	−0·01	−0·03	+0·01	+0·01
2·0	0	0	0	−0·01	—	0	—	0	—
3·0	—	—	0	0	—	0	—	0	—
4·0	—	—	0	0	—	0	—	0	—
5·0	—	—	0	0	—	0	—	0	—
6·0	—	—	—	—	—	—	—	—	—

y \ x	1·0.	0·5.	0	−0·05.	−1·0.	−1·5.	−2·0.	−2·5.	−3·0.
0·4	—	—	—	—	—	—	−0·04	+0·12	−0·09
0·5	−0·02	+0·01	+0·10	+0·17	+0·08	+0·02	−0·06	+0·01	−0·02
0·6	−0·10	−0·09	+0·03	+0·08	+0·01	−0·04	−0·03	−0·02	0
0·7	−0·01	−0·01	−0·04	−0·04	−0·06	−0·04	−0·01	−0·04	−0·02
0·8	0	−0·03	+0·01	−0·04	−0·03	−0·02	−0·01	−0·02	−0·02
0·9	0	−0·01	+0·01	0	0	−0·01	−0·01	−0·01	−0·02
1·0	−0·02	0	0	0	0	−0·01	−0·01	−0·01	−0·02
2·0	0	—	0	—	−0·01	—	0	—	+0·01
3·0	0	—	0	—	0	—	0	—	+0·01
4·0	0	—	0	—	0	—	0	—	0
5·0	0	—	0	—	0	—	0	—	0
6·0	0	—	0	—	0	—	0		0

The Stream Function.

The fundamental assumption upon which comparison between experiment and mathematical theory depends is that the motion of the fluid is wholly two-dimensional. If it is not then either there is eddying in a direction perpendicular to the xy plane or there is a steady streaming in that direction. If the motion were not steady a number of photographs would exhibit differences, but the mean of a number of velocity determinations would eliminate the effect of such eddying. Examination of the velocity

distribution curves shows that the deviations are no larger than the velocities due to the residual motion. If there were steady streaming in a direction at right angles to the xy plane, the effect would be shown in the observed values of $\partial u/\partial x + \partial v/\partial y$ not being zero. These, Table III, are random in magnitude and are no larger than the effect produced by residual motion, and by experimental errors in the differentiation of the curves $u - x$, $v - y$. It therefore follows that there exists a stream function defined as in equation (9) by

$$u = -\frac{\partial \psi}{\partial y}, \quad v = +\frac{\partial \psi}{\partial x},$$

so that

$$\psi_{x=\text{const.}} = -\int u\,dy + \text{C} \text{ or } \psi_{y=\text{const.}} = +\int v\,dx + \text{C}'. \quad . \quad . \quad . \quad . \quad (24)$$

Since the boundary conditions have been chosen so as to transform the problem to one of fluid streaming past the ellipse (a velocity -1 in the x direction having been imposed on the system) to obtain the instantaneous stream function corresponding to the actual physical conditions, the function $-y$ is added to the stream function of equation (24). The distribution of y in the field was found from $\psi_{x=\text{const.}} = -\int u\,dy - y + c$, the constant being such as to make $\psi = -y$ on the cylindrical boundary.

As a check on the distribution of ψ so determined, $\psi_{y=\text{const.}} = \int v\,dx + c'$ was found along a number of contours and these values agreed closely with those determined by the previous integration, thus forming an additional check on the assumption that the flow was two-dimensional.

The streamlines $\psi = \text{const.}$ were then drawn, and are shown in fig. 6. The curves

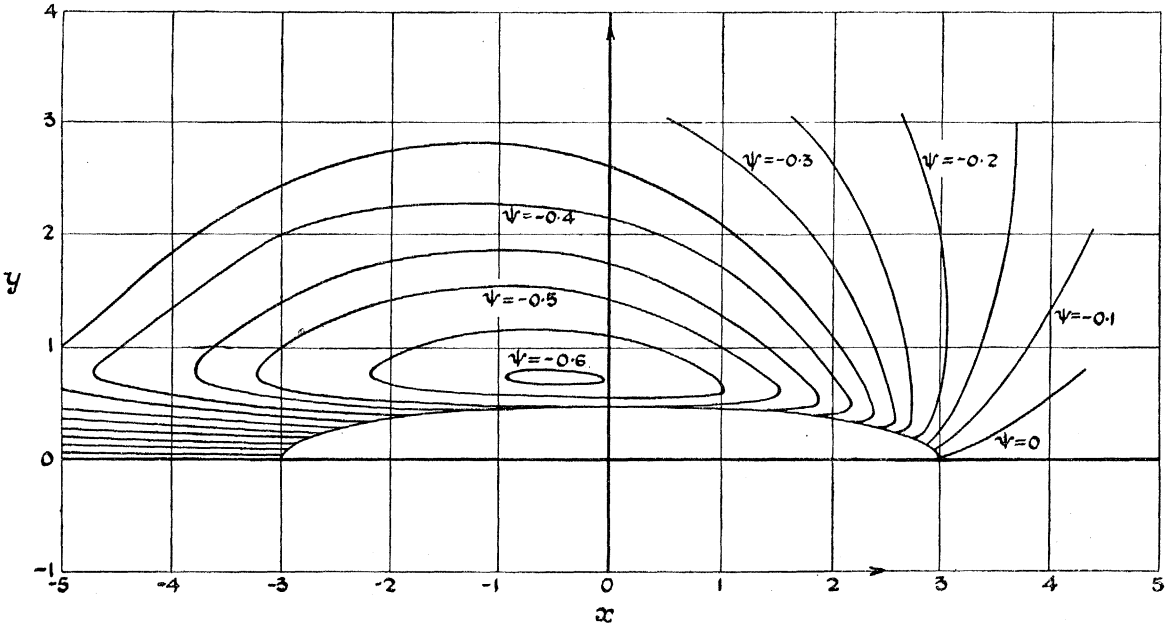

FIG. 6.—Instantaneous stream lines.

from their very nature closely resemble the photographs of the traces of the particles, and in those regions where u and v were not measured the photographs were used for completing the curves.

Determination of the Integrals X *and* Y.

The functions

$$\mathrm{X} = 1/\pi \iint v \frac{\partial v}{\partial y} \frac{\partial \theta}{\partial y} \, dx \, dy,$$

and

$$\mathrm{Y} = 1/\pi \iint v \frac{\partial u}{\partial y} \frac{d\theta}{\partial x} \, dx \, dy$$

are respectively of the form

$$\iint f(x, y) \frac{\partial \theta}{\partial y} \, dx \, dy$$

and

$$\iint g(x, y) \frac{\partial \theta}{\partial x} \, dx \, dy$$

where f and g are functions of x and y, and the integrals taken over the whole field. Consider

$$\mathrm{I} = \iint f(x, y) \frac{\partial \theta}{\partial y} \, dx \, dy = \iint f(x, y) \, d\theta_{x = \text{const.}} \, dx.$$

This is integrable in two stages, first a function $\mathrm{F}(x)$ is determined, where

$$\mathrm{F}(x) = \int f(x, y) \, d\theta_{x = \text{const.}}$$

and this is further integrated with respect to x giving the integral $\mathrm{I} = \int \mathrm{F}(x) \, dx$.

For the determination of $\mathrm{F}(x)$ an integrator devised by Professor L. Bairstow was used. It is a celluloid plate fixed at the point at which the integral is to be found (0), fig. 7, and capable of rotation about that point. In a groove CD slides a carriage, parallel to the radius OR, and carrying a planimeter wheel whose axis of rotation is also parallel to OR. The position of the carriage and wheel relative to 0 is indicated by a linear scale. It will be seen that when the instrument is rotated through a small angle $\partial\theta$ the planimeter wheel will record a magnitude proportional to $r\partial\theta$ where r is the projection of the distance between the wheel and 0, on to OR. If then the values of the function $f(x, y)$ are written along the line AB (a line $x =$ const.), the instrument rotated so that the radius OR traverses the line AB, the carriage at the same time being moved so that r is proportional to the value of $f(x, y)$ at the point of intersection of OR and AB, the planimeter wheel will record a number proportional to

$$\mathrm{F}(x) = \int f(x, y) \, d\theta_{x = \text{const.}}$$

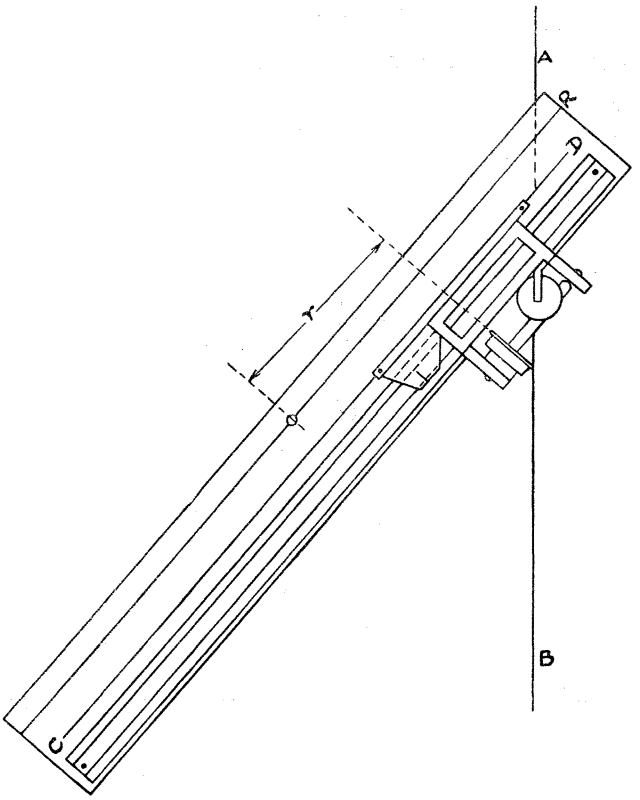

FIG. 7.—Integrator used for the determination of x and y.

TABLE IV.

$$\left(uv - \frac{1}{R}\zeta\right) - X - Y = H \text{ on the Contour.}$$

θ°.	$uv - \frac{1}{R}\zeta$.	− X.	− Y.	H.	θ°.	$uv - \frac{1}{R}\zeta$.	−X.	− Y.	H.
0	0	0	0	0	90	−0·035	0	+0·034	−0·001
5	−0·066	+0·006	+0·043	−0·017	95	−0·019	0	+0·023	+0·004
10	−0·165	+0·010	+0·085	−0·070	100	−0·004	0	+0·011	+0·007
15	−0·279	+0·013	+0·122	−0·144	105	+0·012	0	0	+0·012
20	−0·306	+0·016	+0·148	−0·142	110	+0·026	0	−0·011	+0·015
25	−0·314	+0·018	+0·160	−0·136	115	+0·037	0	−0·021	+0·016
30	−0·308	+0·019	+0·162	−0·127	120	+0·045	0	−0·030	+0·015
35	−0·293	+0·017	+0·160	−0·116	125	+0·050	0	−0·037	+0·013
40	−0·264	+0·014	+0·156	−0·094	130	+0·062	0	−0·039	+0·013
45	−0·234	+0·010	+0·147	−0·077	135	+0·047	0	−0·035	+0·013
50	−0·206	+0·009	+0·135	−0·062	140	+0·037	0	−0·024	+0·012
55	−0·181	+0·007	+0·124	−0·050	145	+0·021	0	−0·009	+0·012
60	−0·156	+0·005	+0·112	−0·039	150	+0·006	0	+0·004	+0·010
65	−0·135	+0·002	+0·101	−0·032	158	−0·001	0	+0·003	+0·002
70	−0·115	+0·001	+0·089	−0·025	160	−0·001	0	+0·002	+0·001
75	−0·094	0	+0·075	−0·019	165	0	0	+0·001	+0·001
80	−0·073	0	+0·061	−0·012	170	0	0	0	0
85	−0·053	0	+0·047	−0·006	175	0	0	0	0

After this process has been carried out along a number of lines $x = \text{const.}$, the integral $I = \int F(x)\, dx$ is evaluated either by summation or by integration of the curve $F(x)$ plotted against x. The method of determining $J = \int (x, y) \frac{\partial \theta}{\partial x}\, dx\, dy$ is similar except that an intermediate integral $G(y) = \int g(x, y)\, d\theta_{y = \text{const.}}$ is found and then $J = \int G(y)\, dy$.

In this way the integrals X and Y were determined at a number of points on an arbitrarily chosen contour defined by $x = 3{\cdot}12 \cos \theta$, $y = 1 \sin \theta$, an ellipse confocal with the boundary; and the distribution of $\left(uv - \frac{1}{R}\zeta\right)$ having also been found on this contour, the value of H upon it, where $H = \left(uv - \frac{1}{R}\zeta\right) - X - Y$, was found as a function of θ.

Determination of the Harmonic Function H_c.

A harmonic function is determinate when known on two contours provided that it is holomorphic. In the present case the experimentally determined value of H on a contour enclosing the ellipse together with the fact that H is zero at infinity, the presence and effect of the walls being ignored, served to define H_c throughout the field, for as the flow of fluid past the elliptic cylinder is symmetrical, there is no circulation and H is a function, single valued and asymmetric with respect to the Ox axis.

By means of a conformal transformation the value of H_c on the boundary ellipse was found from that on the contour, and applying a method due to Bairstow,* a suitable distribution of sources and sinks was found on the boundary satisfying the boundary value of H_c, and necessarily satisfying the contour value, such that by a single integration of this distribution round the boundary the value of H_c could be determined at any desired point of the field.

The conformal transformation $\frac{Z}{2{\cdot}958} = \cosh \log. \frac{Z'}{0{\cdot}845}$ where $Z = x + iy$ and $Z' = x' + iy'$, transforms a point (x, y) in the Z plane to one (x', y') in the Z′ plane so that if

$$x = \left(1{\cdot}75\, r + \frac{1{\cdot}25}{r}\right) \cos \theta$$

and

$$y = \left(1{\cdot}75\, r - \frac{1{\cdot}25}{r}\right) \sin \theta \qquad \ldots\ldots\ldots\ldots \quad (25)$$

then

$$x' = r \cos \theta$$

and

$$y' = r \sin \theta. \qquad (26)$$

* Bairstow and Berry, 'Proc. Roy. Soc.,' A, vol. 95, p. 457 (1919).

The boundary ellipse $\frac{x^2}{3^2} + \frac{y^2}{0{\cdot}5^2} = 1$ in the Z plane transforms into unit circle in the Z′ plane, and the contour ellipse $\frac{x^2}{(3{\cdot}12)^2} + \frac{y^2}{1^2} = 1$ into a circle of radius 1·178 in that plane.

Now H_c was known on the contour ellipse in the Z plane, as a function of θ. It was transformed by the relations (25) and (26), to the contour circle in the Z′ plane, and expanded as a half range asymmetric Fourier series.

$$a_1 \sin\theta + a_2 \sin 2\theta + \ldots a_n \sin n\theta + \ldots \quad \ldots\ldots\ldots\ldots \quad (27)$$

But in the Z′ plane a single valued harmonic function zero at infinity and asymmetric in y' may be represented as a series

$$\frac{A_1}{r}\sin\theta + \frac{A_2}{r^2}\sin 2\theta + \ldots \frac{A_n}{r_n}\sin n\theta + \ldots, \quad \ldots\ldots \quad (28)$$

so that H_c on the contour is

$$\frac{A_1}{1{\cdot}178}\sin\theta + \frac{A_2}{(1{\cdot}178)^2}\sin 2\theta \ldots \frac{A_n}{(1{\cdot}178)^n}\sin n\theta \ldots, \quad \ldots\ldots \quad (29)$$

hence

$$A_1 = 1{\cdot}178\, a_1,\ A_2 = (1{\cdot}178)^2\, a_2 \ldots A_n = (1{\cdot}178)^n\, a_n; \quad \ldots\ldots \quad (30)$$

whence it follows that on the boundary

$$H_c = 1{\cdot}178\, a_1 \sin\theta + (1{\cdot}178)^2\, a_2 \sin 2\theta \ldots (1{\cdot}178)^n\, a_n \sin n\theta. \quad \ldots\ldots \quad (31)$$

Transforming to the Z plane, the value of H_c was thus found on the boundary ellipse, and known also as an analytic expression at any point of the field. This expression was, however, inconvenient in use, and a distribution of sources and sinks was found on the boundary.

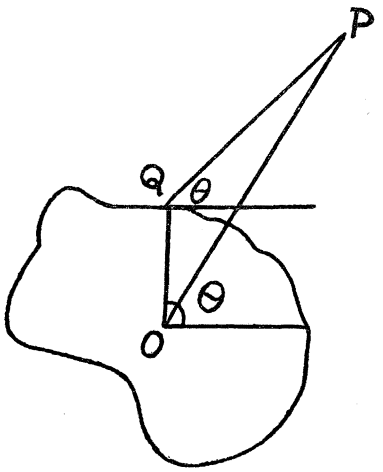

FIG. 8

Suppose $d\chi$ to be an elementary source at a point Q of the boundary, then the contribution of $d\chi$ to the harmonic function H_c^P at P is

$$\frac{1}{2\pi}\theta d\chi,$$

hence

$$H_c^P = \frac{1}{2\pi}\int \theta d\chi, \quad \ldots\ldots \quad (32)$$

the integral being taken round the boundary. It may be shown that

$$H_c^P = -\frac{1}{2\pi}\int \chi_Q\, d\theta, \quad \ldots\ldots\ldots\ldots \quad (33)$$

indeterminate to a constant and that

$$\tfrac{1}{2}\chi_Q = H_c^Q + \frac{1}{\pi}\int_\Theta^{\Theta+\Pi} H_c^Q\, d\theta + \frac{1}{\pi^2}\iint_\Theta^{\Theta+\Pi} H_c^Q\, d\theta\, d\theta_1 + \ldots \quad \ldots \quad (34)$$

where H_c^Q is the value of H_c at Q, each integral being taken for Q travelling round the boundary, but the radius vector traversing only an angle π. The double integral signifies that the operation is repeated on the result of the first. In the present work the indeterminate constant vanishes since both H_c and χ are asymmetric in y. The integration was conveniently carried out with the integrator described above. The method is similar to that by which X and Y were determined, the radius vector OR, in this case, traversing the boundary whilst at the same time the distance r is made proportional to the value of H_c^Q, $1/\pi \int H_c^Q\, d\theta$ etc. at the point of intersection of OR and the boundary.

The experimentally determined value of H on the contour, Table IV, was analysed into a Fourier Series of twelve terms, its value being

$$-0{\cdot}0279 \sin\theta - 0{\cdot}0557 \sin 2\theta - 0{\cdot}0415 \sin 3\theta - 0{\cdot}0262 \sin 4\theta - 0{\cdot}0200 \sin 5\theta - 0{\cdot}0122 \sin 6\theta - 0{\cdot}0069 \sin 7\theta - 0{\cdot}0026 \sin 8\theta - 0{\cdot}0026 \sin 9\theta - 0{\cdot}0009 \sin 10\theta - 0{\cdot}0010 \sin 11\theta$$

whence by equation (30) the boundary value was

$$H_c^Q = -0{\cdot}0328 \sin\theta - 0{\cdot}0772 \sin 2\theta - 0{\cdot}0678 \sin 3\theta - 0{\cdot}0505 \sin 4\theta - 0{\cdot}0453 \sin 5\theta - 0{\cdot}0326 \sin 6\theta - 0{\cdot}0217 \sin 7\theta - 0{\cdot}0092 \sin 8\theta - 0{\cdot}0113 \sin 9\theta - 0{\cdot}0047 \sin 10\theta - 0{\cdot}0058 \sin 11\theta.$$

In order to apply the integral equation (34), the successive functions

$$\frac{1}{\pi}\int H_c^Q\, d\theta, \quad \frac{1}{\pi^2}\iint H_c^Q\, d\theta\, d\theta_1, \text{ etc.},$$

of the series were determined, and being rapidly convergent were found to be negligible beyond the sixth term. The resulting distribution of $\frac{1}{2}\chi_Q$ when integrated round the boundary gave a value of H_c, where $H_c = -\frac{1}{2\pi}\int \chi_Q\, d\theta$, at any point of the field, and on comparison of the value of H_c so determined with the original on the contour, the agreement was seen to be poor in the region $\theta = 0°$ to $20°$ as the number of terms in the Fourier analysis of H_c had been too small. A small correction to $\frac{1}{2}\chi_Q$ was therefore necessary, and a linear distribution of sources and sinks was assumed to exist on the boundary between the points $-22{\cdot}5$ to $-17{\cdot}5°$, $-17{\cdot}5$ to $-12{\cdot}5°$, $-12{\cdot}5$ to $-7{\cdot}5°$, $-7{\cdot}5$ to $-2{\cdot}5°$, $-2{\cdot}5$ to $2{\cdot}5°$, $2{\cdot}5$ to $7{\cdot}5°$, $7{\cdot}5$ to $12{\cdot}5°$, $12{\cdot}5$ to $17{\cdot}5°$, $17{\cdot}5$ to $22{\cdot}5°$, the line density on each element being unknown, and

assigned values $-w$, $-x$, $-y$, $-z$, 0, $+z$, $+y$, $+x$, $+w$ respectively. The contribution of each such element to the value of H_c at four points on the contour was found, and solving simultaneous equations of four unknowns, a distribution was found such that when added to the former distribution of $\frac{1}{2}\chi_Q$ the resulting integral $-\frac{1}{2\pi}\int \chi_Q \, d\theta$ coincided with the original value of H_c and H on the contour. The comparison is shown in Table V and diagrammatically in fig. 9.

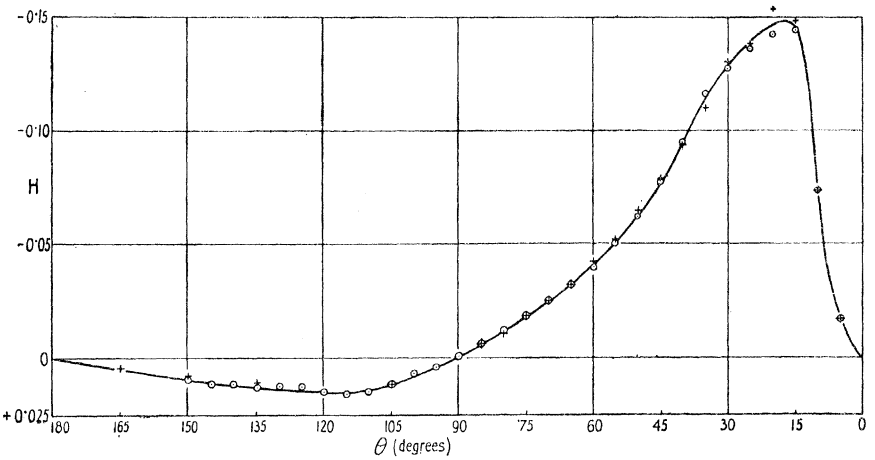

FIG. 9.—Distribution of H and H_c on the contour. $\odot = H$; $+ = H_c = -\frac{1}{2}\pi \int \chi_Q d\theta$.

TABLE V.

θ°.	H_cQ.	$\frac{1}{2}\chi_Q$.	On the contour. H.	On the contour. $H_c = -\frac{1}{2\pi}\int \chi_Q d\theta$.	θ°.	H_cQ.	$\frac{1}{2}\chi_Q$.	On the contour. H.	On the contour. $H_c = -\frac{1}{2\pi}\int \chi_Q d\theta$.
0	0	0	0	0	60	−0·030	−0·009	−0·039	−0·042
5	−0·121	−0·025	−0·017	−0·017	65	−0·024	−0·007	−0·032	−0·032
10	−0·212	−0·205	−0·070	−0·073	70	−0·021	−0·007	−0·025	−0·025
15	−0·256	−0·201	−0·144	−0·148	75	−0·020	−0·010	−0·019	−0·018
20	−0·254	−0·190	−0·142	−0·153	80	−0·015	−0·007	−0·012	−0·011
25	−0·222	−0·163	−0·136	−0·138	85	−0·005	0	−0·006	−0·006
30	−0·180	−0·122	−0·127	−0·130	90	+0·006	+0·007	−0·001	0
35	−0·140	−0·086	−0·116	−0·110	105	+0·024	+0·019	+0·012	+0·012
40	−0·107	−0·059	−0·094	−0·093	120	+0·024	+0·017	+0·015	+0·015
45	−0·084	−0·045	−0·077	−0·078	135	+0·013	+0·010	+0·013	+0·011
50	−0·062	−0·029	−0·062	−0·064	150	+0·016	+0·012	+0·010	+0·008
55	−0·043	−0·017	−0·050	−0·052	165	−0·006	+0·007	+0·001	+0·004

Comparison of H_c *with* H.

A satisfactory distribution of $\frac{1}{2}\chi_Q$ having been found, it was possible to determine the value of H_c at any point, or along any contour of the field, and to compare it with the experimental value of H at that point. The distribution was satisfactory in that the value of the harmonic function H_c obtained from it coincided with the distribution of H along the particular contour $\frac{x^2}{(3\cdot12)^2} + y^2/1 = 1$, so that a comparison of H with H_c at any point not on that contour formed a criterion of the agreement of experiment with theory.

The comparison between H and H_c was made along three lines $y = +0\cdot75$, $x = +3\cdot0$, and $x = -2\cdot0$, and the results are shown below in Table VI, and also in fig. 10.

TABLE VI.

$y = +0\cdot75$.						$x = +3\cdot0$.		
x.	H.	$H_c = -\frac{1}{2\pi}\int\chi_Q d\theta$.	x.	H.	$H_c = -\frac{1}{2\pi}\int\chi_Q d\theta$.	y.	H.	$H_c = -\frac{1}{2\pi}\int\chi_Q d\theta$.
4	−0·025	−0·025	1·50	−0·034	−0·034	+2	−0·010	−0·018
3·75	−0·033	−0·033	1·25	−0·025	−0·025	+1·5	−0·016	−0·023
3·5	−0·047	−0·047	1·0	−0·021	−0·021	+1·0	−0·028	−0·034
3·25	−0·063	−0·063	0·75	−0·018	−0·018	+0·75	−0·040	−0·040
3·0	−0·078	−0·080	0·5	−0·011	−0·011	+0·25	−0·090	−0·090
2·75	−0·095	−0·090	0·25	−0·006	−0·004			
2·5	−0·093	−0·089	−0·5	+0·004	+0·014	$x = -2\cdot0$.		
2·25	−0·081	−0·077	−1·0	+0·010	+0·020			
2·0	−0·065	−0·065	−1·5	+0·013	+0·020	+2·0	+0·014	+0·010
1·75	−0·050	−0·050	−2·0	+0·015	+0·015	+1·5	+0·015	+0·012
						+1·0	+0·015	+0·014
						+0·5	+0·016	+0·016

It will be seen that agreement between H and H_c is close along the line $y = 0\cdot75$ from $x = 4$ to 0, and along $x = 3$ from the boundary to $y = 0\cdot8$, but that beyond these points, however, there are deviations which may arise from

(1) experimental error,
(2) the viscous equations being invalid,
(3) the flow not being two-dimensional,
(4) the presence of the boundary walls, or
(5) the presence of the oscillating wake.

The experimental errors arising in the course of the experiments were certainly not as great as the differences between H and H_c, and were probably less than 0·004.

Such errors would be found in front of and near to the cylinder where H is the difference between large numerical values of $X + Y$ and $uv - \frac{1}{R}\zeta$, rather than in those regions where deviations actually occur. The viscous equations for steady flow have been proved for flow through pipes of various cross-section and have been found to be valid. The possibility of the flow not being two-dimensional has been discussed previously and determinations of $\partial u/\partial x + \partial v/\partial y$ and of the stream function demonstrate that the flow is two-dimensional.

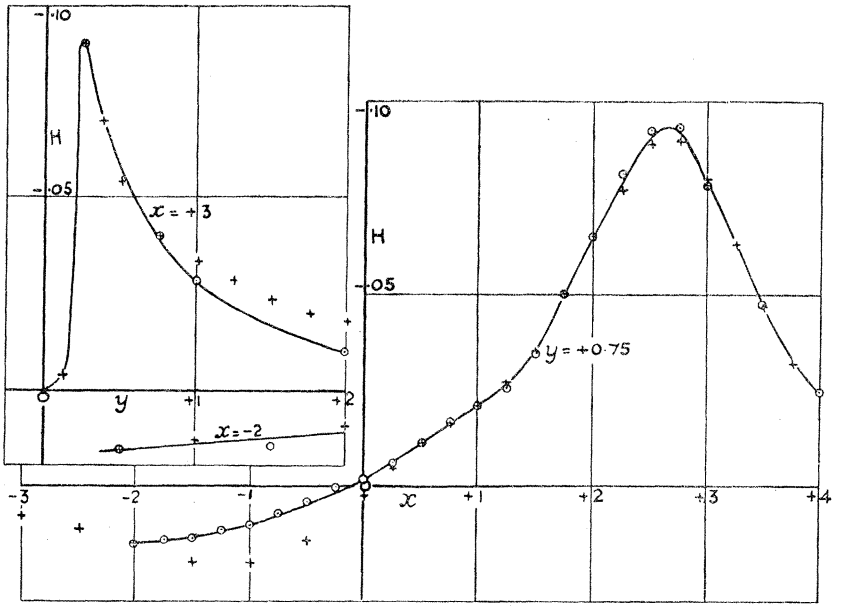

FIG. 10.—Distribution of H and H_c on lines $y = +0{\cdot}75$, $x = +3{\cdot}0$, and $x = -2{\cdot}0$, $\odot = H$; $+ = H_c$.

The disparity between H and H_c is then due to the presence of the boundary walls, and of the oscillating wake.

Since the boundary walls were the same distance apart when either cylinder was in the tank, their distance from the cylinder in non-dimensional units was not the same for each. The conditions of flow then were neither strictly identical nor identical with the conditions of flow in an infinite fluid; *e.g.*, on a line $y = 1{\cdot}5$ there were differences in the value of v determined with each cylinder of $0{\cdot}005$. Now H_c is a harmonic function tending to zero at infinity whereas H becomes very small at the outer boundary of the fluid. It will be seen then that the rate of decrease outward of H_c is less than that of H, a fact which is clearly apparent in fig. 10, in the inset along $x = +3{\cdot}0$.

As the wake was oscillating the region behind $x = -3{\cdot}0$ was neglected in the present work owing to the difficulty of timing the photography so as to obtain a set of photographs of the wake at any one phase of oscillation. Now the functions X and Y in the equation

$$\left(uv - \frac{1}{R}\zeta\right) - H = X + Y$$

are integrals over the whole field with respect to a point under consideration, so that any part of the field neglected must cause some error in the determined values of X and Y. The contribution of the neglected region to the value of X + Y at any point of the field may be divided into two parts, one independent of, and the other a periodic function of time. Since the oscillation of the wake was small for some distance behind the cylinder, the parts of the integrals which were periodic functions of time were probably small in the region forward of $x = -3{\cdot}0$, as experiment shows, but the other parts, independent of time, were not negligible in the region from $x = -3{\cdot}0$ to $x = 0$.

I wish to express my thanks to Professor L. Bairstow, C.B.E., A.R.C.S., F.R.S., for his direction of the work; to the Department of Scientific and Industrial Research for the means whereby the research was undertaken; and to the Rector of the Imperial College of Science and Technology, H. T. Tizard, Esq., C.B., F.R.S., for the extended use of the laboratories at the College until the investigation had been brought to a successful termination.

Summary.

The flow of a viscous fluid past an elliptic cylinder has been compared with mathematical theory and agreement between them has been found to be close [in that region of the field] in the neighbourhood of the front of the cylinder. In the outer field, and towards the back of the cylinder, deviations occurred between theory and experiment owing to the fact that the effects of the boundary walls and of the wake had been neglected. The results obtained, however, justify an extension of the method employed to conditions where the presence of the walls is considered, and where the influence of the eddying wake is taken into account.

PHILOSOPHICAL TRANSACTIONS OF THE ROYAL SOCIETY A MATHEMATICAL, PHYSICAL & ENGINEERING SCIENCES

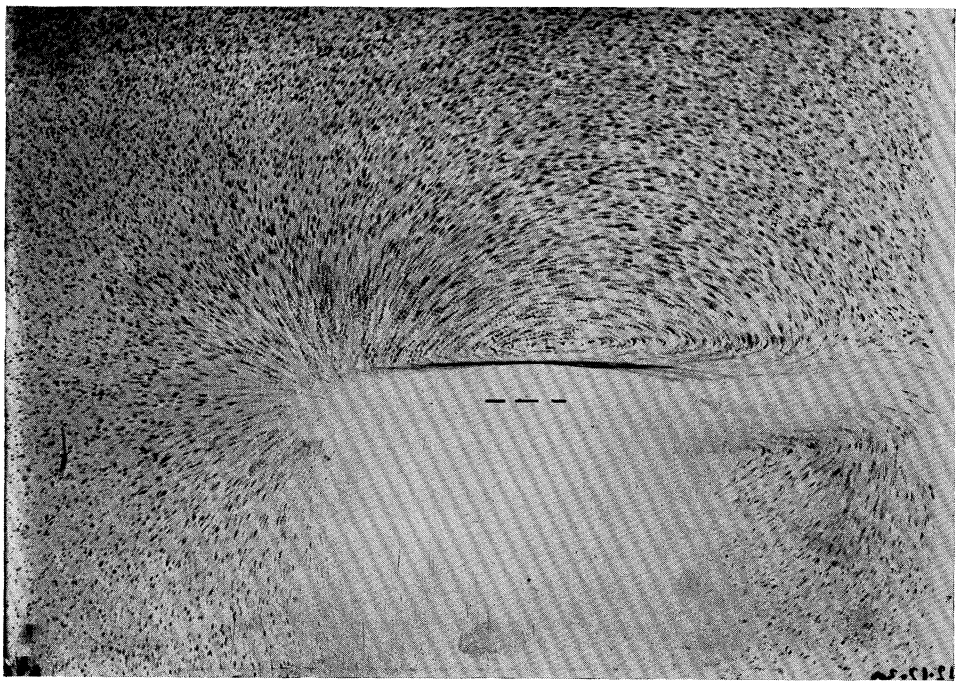

FIG. 11.—Flow in the outer field.
A 21.

FIG. 12.—Flow in front of the cylinder.
C 24.

PHILOSOPHICAL TRANSACTIONS OF THE ROYAL SOCIETY A MATHEMATICAL, PHYSICAL & ENGINEERING SCIENCES

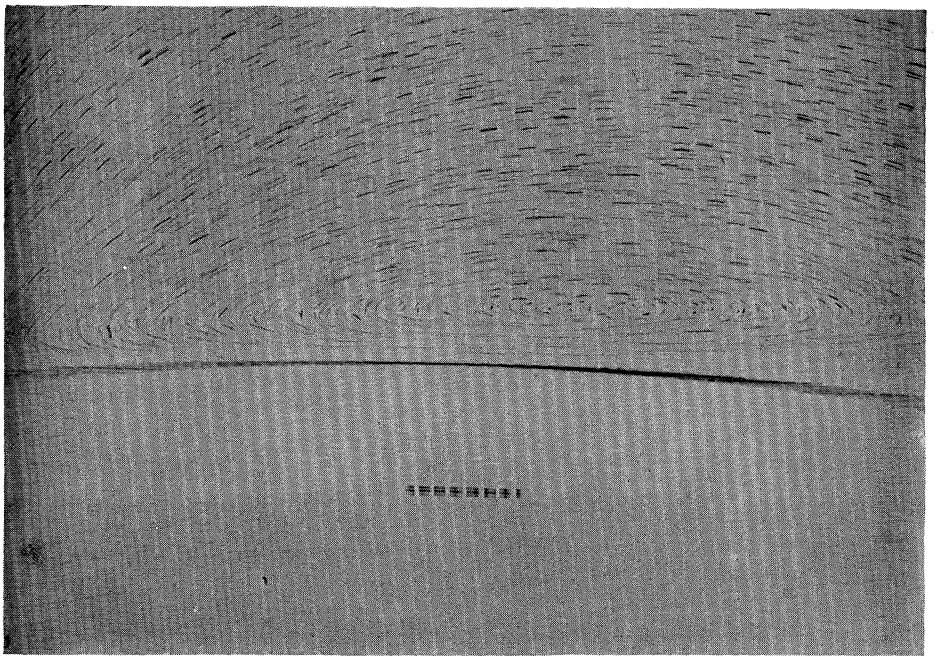

FIG. 13.—Flow over the middle of the cylinder.
C 40.

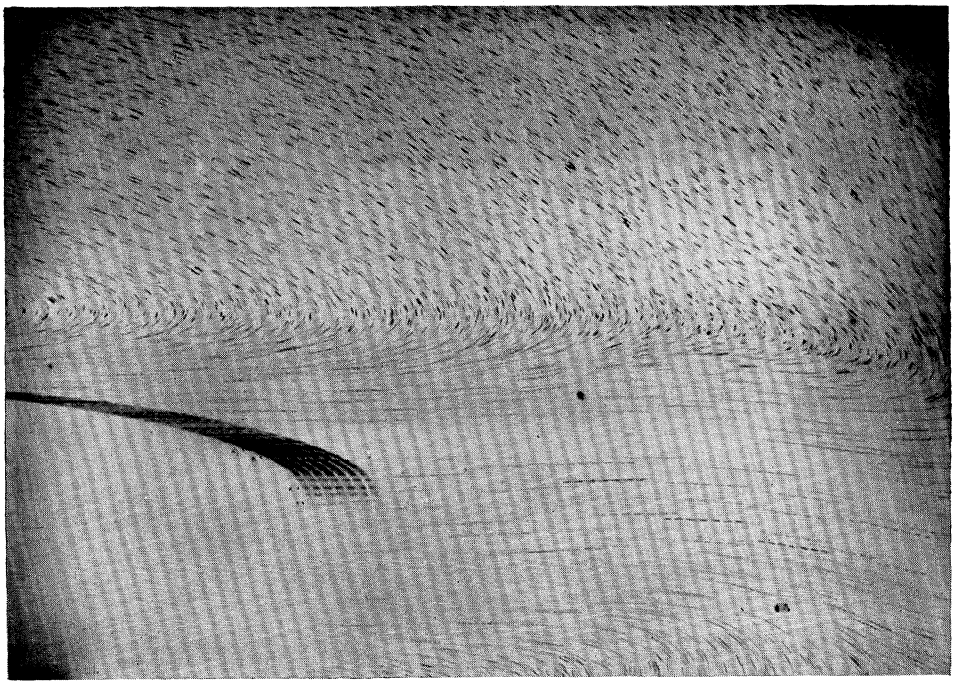

FIG. 14.—Flow behind the cylinder.
C 52.

PHILOSOPHICAL TRANSACTIONS OF THE ROYAL SOCIETY A MATHEMATICAL, PHYSICAL & ENGINEERING SCIENCES

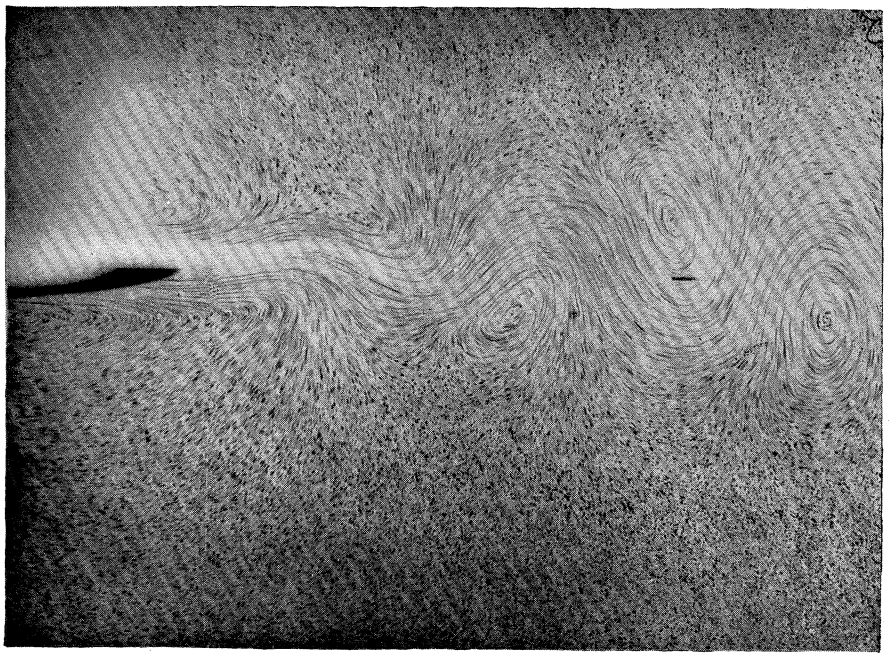

FIG. 15.—Formation of the "Vortex Street."
A 23.

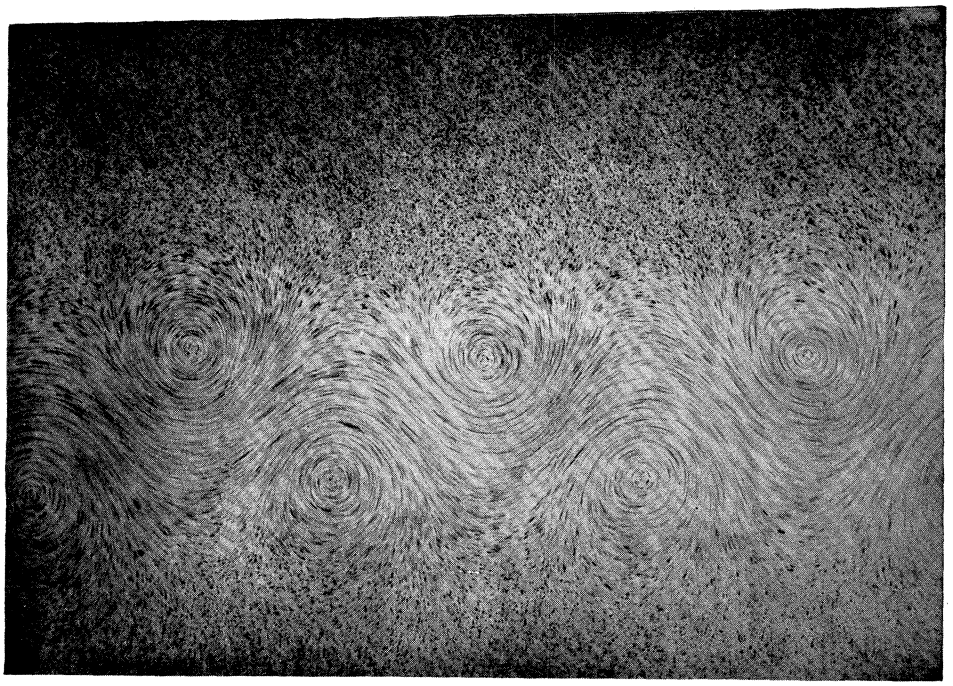

FIG. 16.—"Vortex Street" at a mean distance of 3–$\frac{1}{3}$ chords behind the cylinder.
A 24.

PHILOSOPHICAL TRANSACTIONS OF THE ROYAL SOCIETY A MATHEMATICAL, PHYSICAL & ENGINEERING SCIENCES

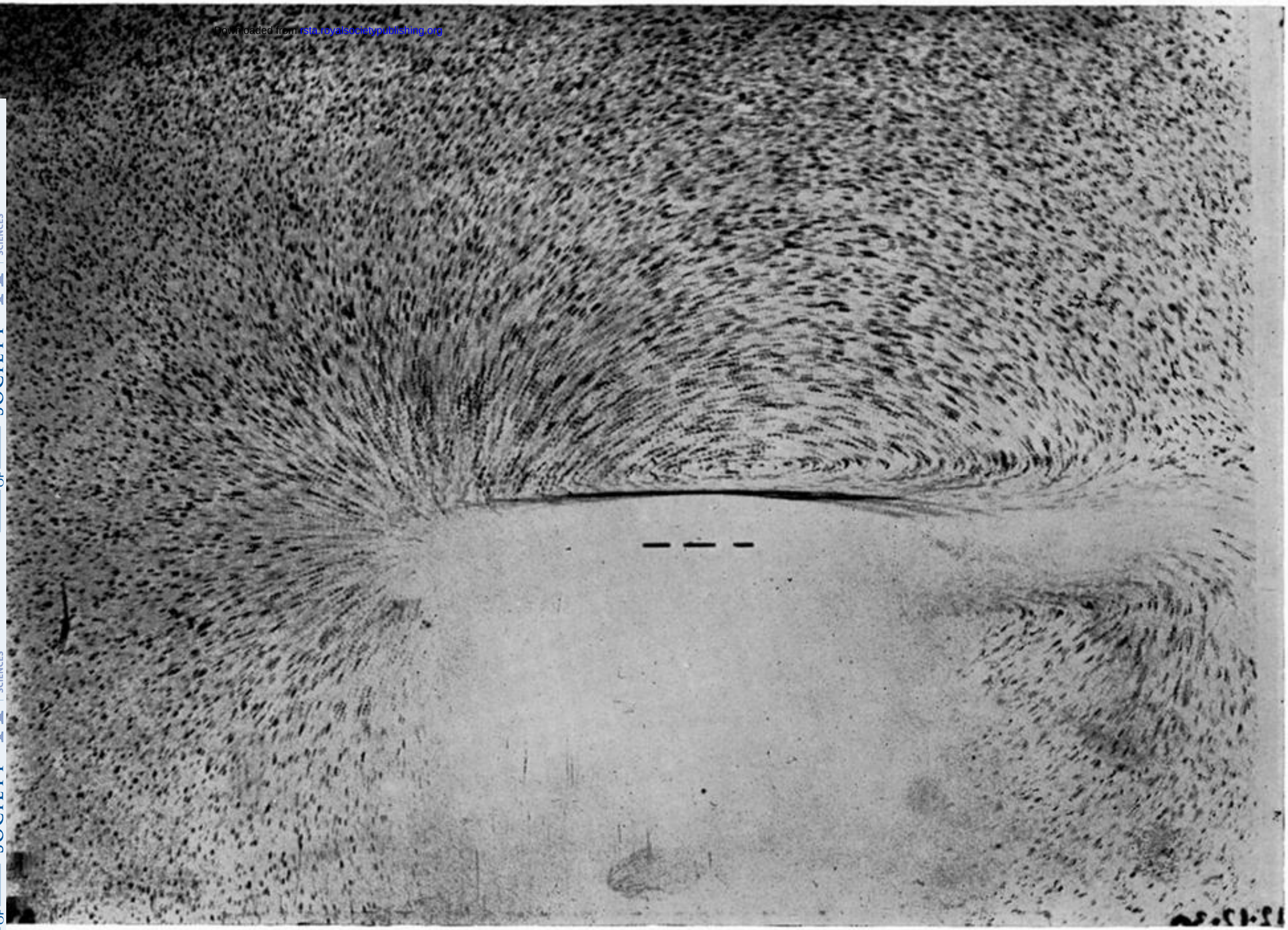

FIG. 11.—Flow in the outer field.

Fig. 12.—Flow in front of the cylinder.

C 24.

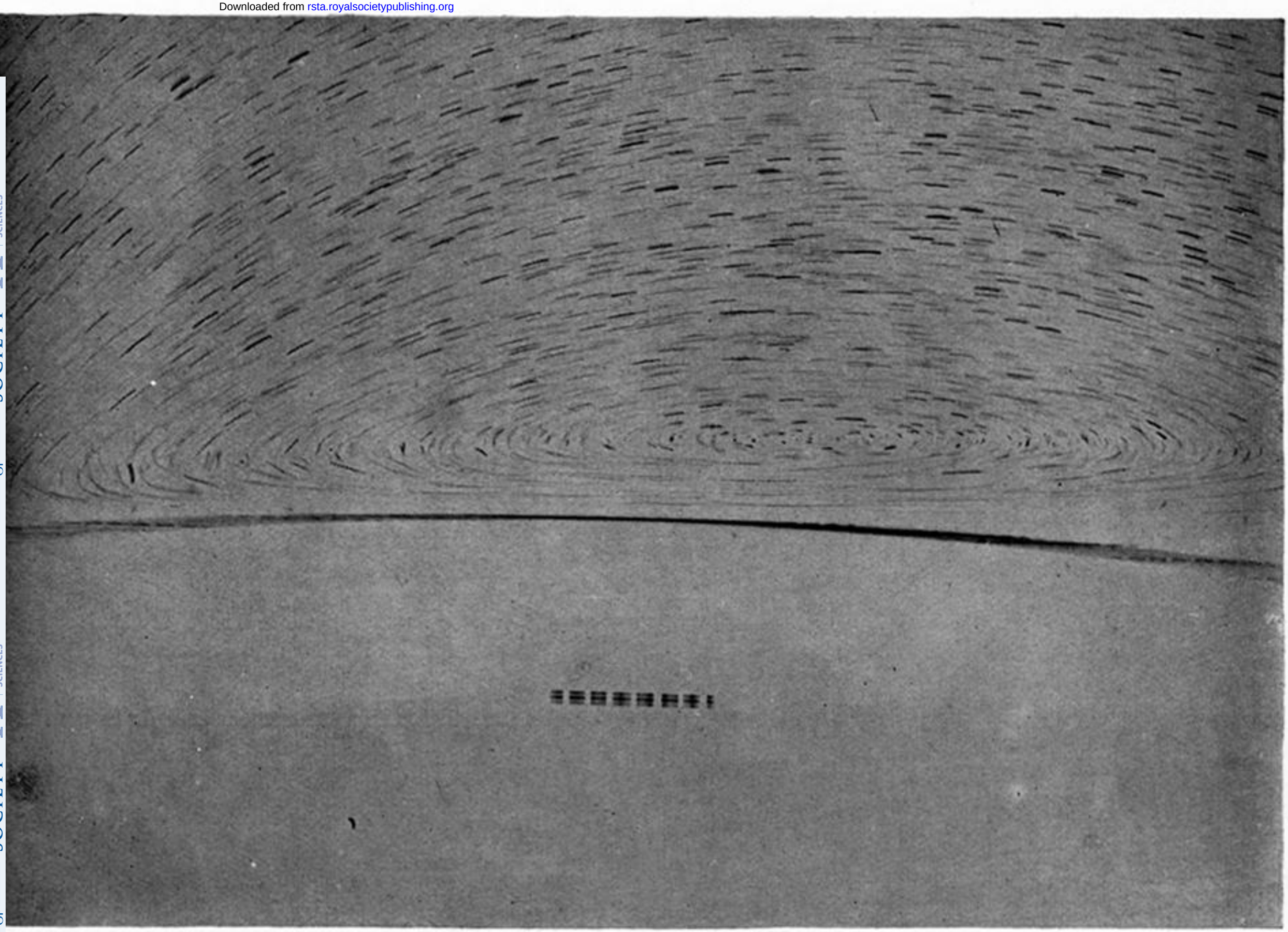

FIG. 13.—Flow over the middle of the cylinder.

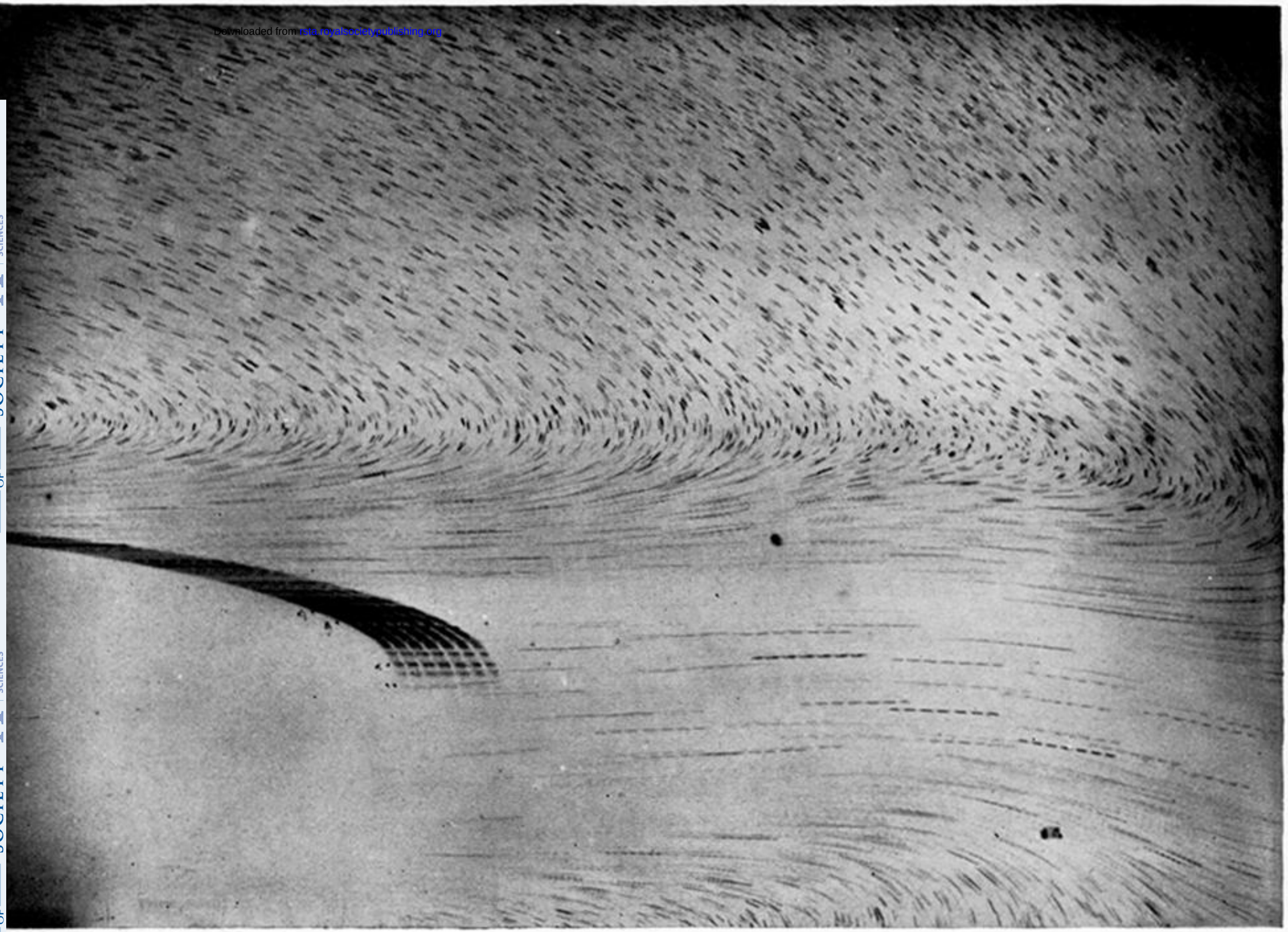

FIG. 14.—Flow behind the cylinder.

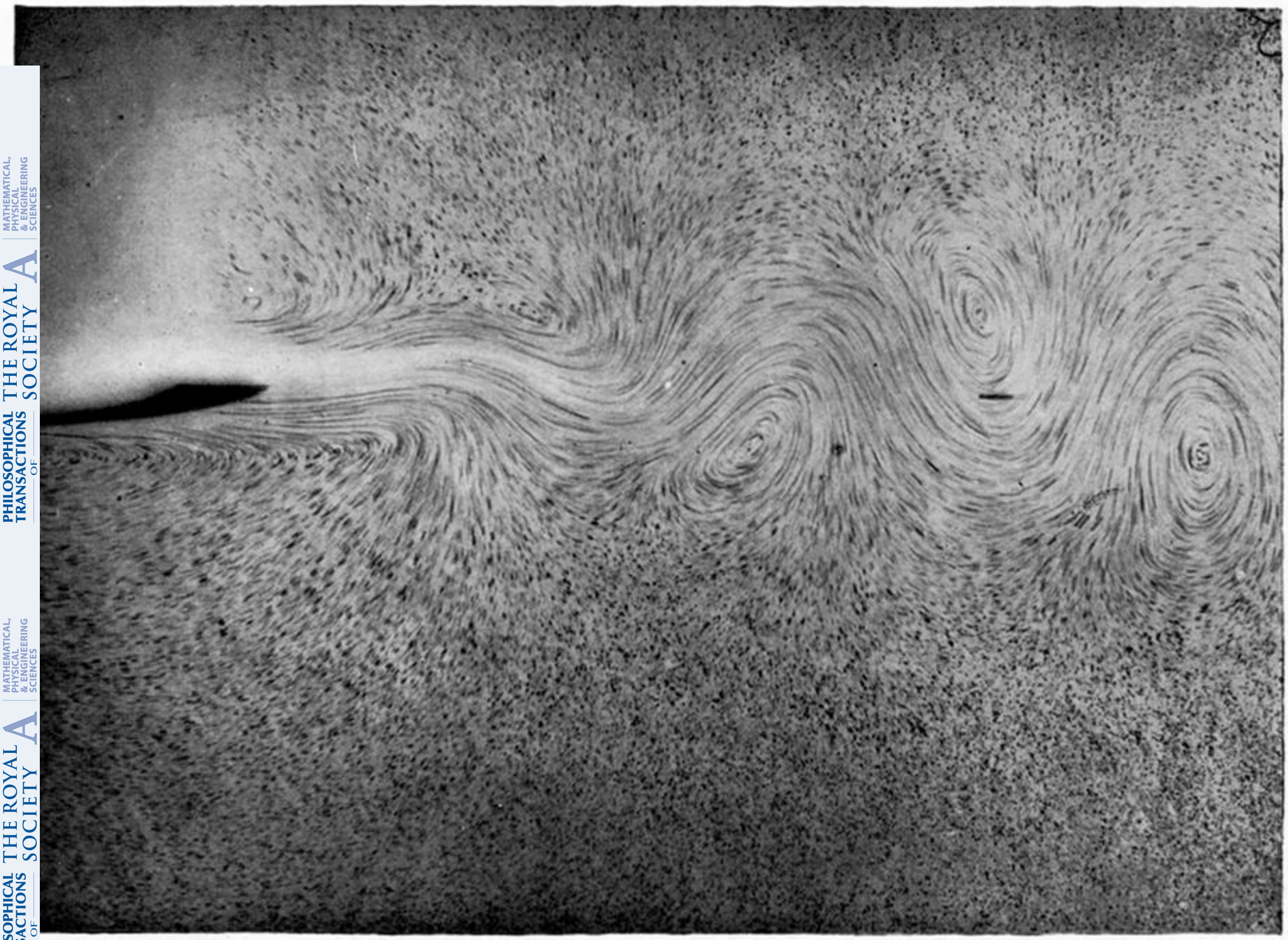

FIG. 15.—Formation of the " Vortex Street."

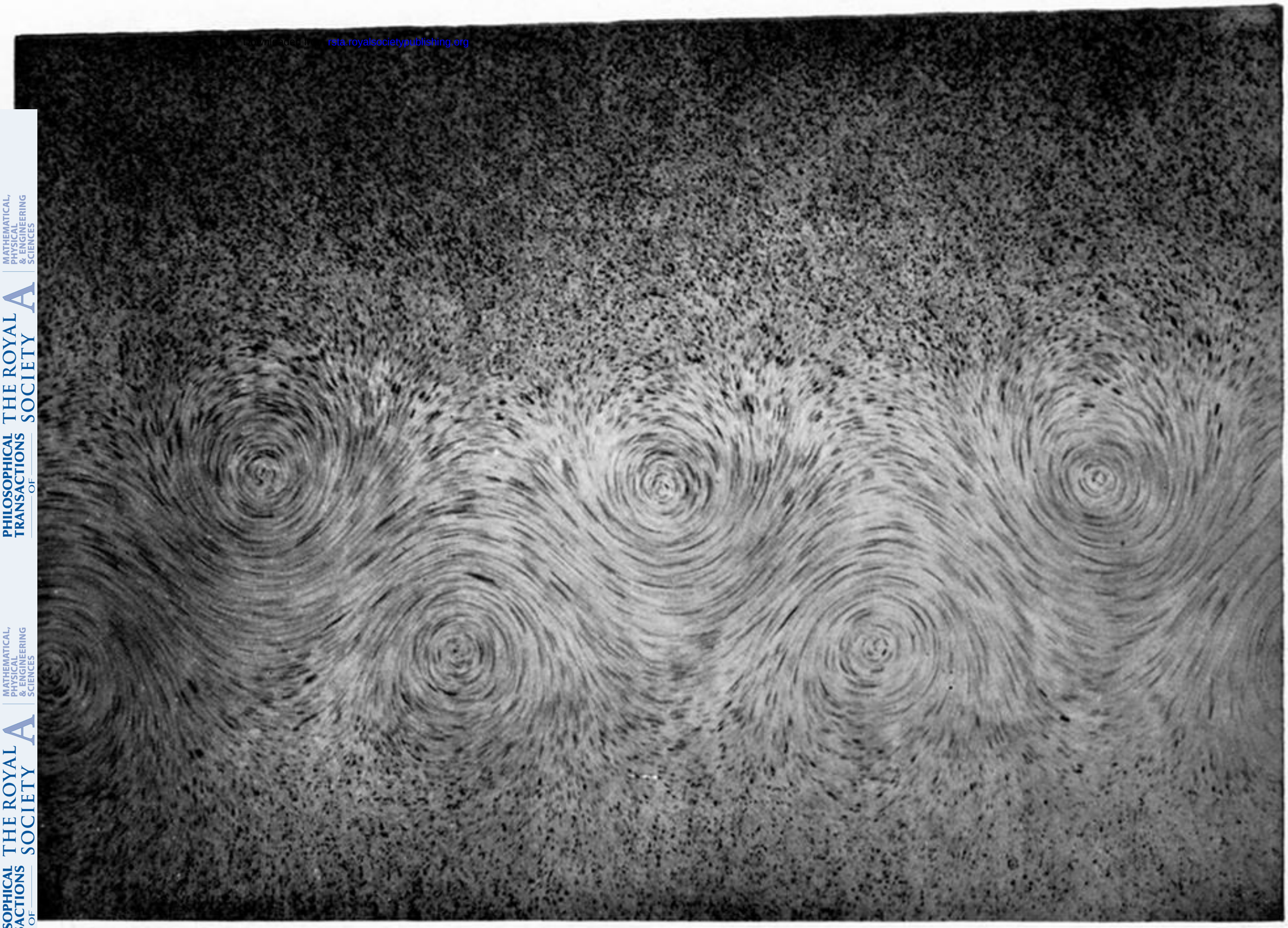

FIG. 16.—" Vortex Street " at a mean distance of 3–$\frac{1}{3}$ chords behind the cylinder.